Degradation of methyl *tertiary*-butyl ether (MTBE) by anodic Fenton treatment

Song Hong [1], Huichun Zhang [2], Christian M. Duttweiler, Ann T. Lemley *

Graduate Field of Environmental Toxicology, TXA, MVR Hall, Cornell University, Ithaca, NY 14853, USA

Abstract

Degradation of MTBE, a common fuel oxygenate, was investigated using anodic Fenton treatment (AFT) and by comparison with classic Fenton treatment (CFT). The AFT system provided an ideal pH environment (2.5–3.5) for the Fenton reaction and utilized gradual delivery of ferrous iron and hydrogen peroxide, which was more efficient than batch CFT to degrade MTBE and its breakdown products. The optimized ratio of ferrous iron to hydrogen peroxide for AFT was determined to be 1:5 (in mmol). Depending on the initial concentration, MTBE was completely degraded by the optimized AFT in 4–8 min. The breakdown products found during the treatment of MTBE were acetone, *t*-butyl formate, *t*-butanol, methyl acetate, acetic acid, and formic acid, which were all completely degraded by the optimized AFT in 32 min. Based on the experimental results and other work reported in the literature, degradation mechanisms of MTBE and its breakdown products in AFT and CFT were proposed. Generally, reactions are initiated by H-abstraction by $^\bullet$OH, generating carbon-centered radicals which undergo various reactions including α/β-scission within the radical, combination with oxygen, oxidation by ferric ion, and reduction by ferrous ion before generating the final oxidation products. Radical combination with oxygen (and the reactions thereafter) and radical oxidation by ferric ion are believed to be the most important pathways in the overall fate of the generated radicals, while radical reduction by ferrous ion is the least important. By elucidating the reaction kinetics and mechanisms of MTBE degradation in the anodic Fenton system, this study offers a potential remediation technique for treating MTBE-contaminated wastewater.
© 2007 Elsevier B.V. All rights reserved.

Keywords: MTBE; Breakdown products; Anodic Fenton treatment (AFT); Hydroxyl radical; Reaction mechanism; Redox reaction with ferrous and ferric ions

1. Introduction

Methyl *t*-butyl ether (MTBE) has been used as a fuel oxygenate for over 20 years [1]. MTBE and other oxygenates increase the efficiency of combustion and decrease the emission of carbon monoxide. They also reduce ozone pollution by partially eliminating the need for ozone-producing aromatic compounds in gasoline [2]. However, MTBE is a risk to human health and is classified by the USEPA as a possible human carcinogen [3]. MTBE spilled to soil has a high potential to leach to groundwater and persist for a long time due to its high water solubility and low biodegradability. MTBE contamination of water is still a significant environmental problem and demands a suitable technology for remediation [4–6].

There are many reports on the degradation of MTBE in the atmosphere, water, and soil. The photo-oxidation of MTBE under atmospheric conditions was investigated using a NO_x–air system [7–9]. Degradation was initiated by either $^\bullet$OH or Cl$^\bullet$ generated from photolysis of alkyl nitrite or chlorine, respectively. Atmospheric photocatalyzed oxidation of MTBE on fly ash was also reported [10], and the degradation potential of MTBE by microorganisms was investigated [11,12]. Kang and Hoffmann [13] investigated oxidation of MTBE by $^\bullet$OH generated from sonolysis of ozone. The degradation products of MTBE by the photo-Fenton process were detected by other researchers [14]. Other reported studies on MTBE treatment used ozone and ozone combined with hydrogen peroxide [15,16], photolysis catalyzed by TiO_2 slurries, ultraviolet photolysis of hydrogen peroxide [17], and a combination of several processes including photocatalysis, H_2O_2 photolysis, and sonolysis [18,19]. Degradation products and reaction pathways of MTBE in water during ultraviolet/hydrogen peroxide treat-

---

ment were intensively investigated [20,21]. Phytoremediation of MTBE was also studied [22]. In addition, MTBE degradation was carried out in classical Fenton treatment, and the reaction kinetics and degradation products were reported for different operating conditions [12,23,24,26,27]. As a variation of the Fenton reaction, Bergendahl and Thies [28] investigated the feasibility of using zero-valent iron as the source of ferrous iron in the Fenton reaction of MTBE.

Most of the reported degradation and treatment of MTBE involved reactions initiated by hydrogen abstraction by $^\bullet$OH, a critical reagent in degrading environmental pollutants in advanced oxidation processes (AOPs) [29]. AOPs are particularly attractive in the remediation of MTBE because of MTBE's high resistance to biodegradation and its weak adsorption to activated carbon. It is also too costly to strip MTBE out of water to be incinerated [17]. Among the AOPs, the Fenton reaction generates $^\bullet$OH by reducing hydrogen peroxide with ferrous ion (reactions (1)–(3)) [30]. There are many reports on the remediation of pollutants by classic Fenton treatment (CFT) where ferrous salt and hydrogen peroxide are used as reagents [12,23–27]:

$$Fe^{2+} + H_2O_2 \rightarrow Fe^{3+} + {}^\bullet OH + OH^-, \qquad k_1 = 76\,M^{-1}\,s^{-1} \tag{1}$$

$$^\bullet OH + MTBE \rightarrow intermediates,$$
$$k_2 = 1.57 \times 10^9\,M^{-1}\,s^{-1}\,[31] \tag{2}$$

$$^\bullet OH + intermediates \rightarrow final\ degradation\ products,$$
$$k_i \approx 10^6\ to\ 10^9\,M^{-1}\,s^{-1}\,[29] \tag{3}$$
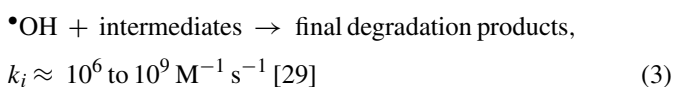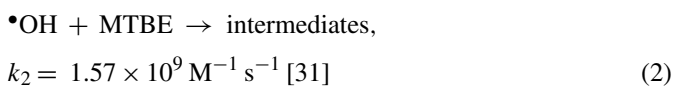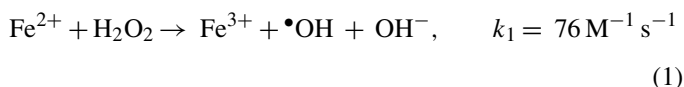
Electrochemical Fenton treatment (EFT), an electrochemical variation of the CFT, was also applied to degrade a variety of pesticides [31–33]. In EFT, ferrous ion is delivered electrochemically from a sacrificial anode made of steel plate (reaction (4)). This eliminates the drawback in CFT that requires handling large quantities of hydrogroscopic salt and maintaining a reduced ferrous salt solution. Hydrogen peroxide is added to a cell containing iron electrodes that function as both anode and cathode. When electrolysis starts, the Fenton reaction takes place. Water is reduced at the cathode, generating hydrogen gas and hydroxide ion and raising the pH to near neutral. Such a pH increase results in the precipitation and/or formation of hydrated colloids from Fe^{3+} and Fe^{2+} ions. Part of the precipitates and colloids will coat the surface of the electrodes, reducing the rates of electrochemical and Fenton reactions:

$$anode: Fe^0 \rightarrow Fe^{2+} + 2e^-, \qquad E^0 = 0.44\,V\,[34] \tag{4}$$

$$cathode: 2H_2O + 2e^- \rightarrow 2OH^- + H_2\,(gas)\,[35] \tag{5}$$

Saltmiras and Lemley [36] developed a novel anodic Fenton treatment (AFT) system that allows the Fenton reaction to occur in an anodic half-cell. The cathode cell and anode cell were connected by a salt bridge. AFT provides an optimum pH (2–3.5) for Fenton treatment. Thus the AFT system eliminates the on-site usage of large quantities of ferrous salts as in CFT and offers the possibility of improving performance over the original electrochemical method.

Most publications on the Fenton reaction accept the Haber and Weiss theory that hydroxyl radical is the actual oxidant in the Fenton reaction [37,38], and this will be used to understand the mechanism in this study. Although some have proposed such oxidants as oxoiron (IV) or (V) species in place of or in addition to $^\bullet$OH as part of the oxidants in the Fenton reaction [39–42], Walling [43] and Macfaul et al. [44] have successfully shown that $^\bullet$OH is the major oxidant. In addition, in the Fenton reaction, the iron species actively reacts with parent compounds and/or intermediates through oxidation, reduction, and coordination, a typical behavior for transition metals in group 8 of the Periodic Table. Thus the degradation pathways should include the reactions with iron species in addition to the ones involving hydroxyl radicals and molecular oxygen, as reported by Walling [30].

The reported break-down products of MTBE in the environment or during pollutant treatments are *t*-butyl formate (TBF), *t*-butyl alcohol (TBA), methyl acetate, and acetone in the classic Fenton system [26]; TBF, TBA, methyl acetate, acetone, peroxidic substances, formaldehyde, alkanes (methane, ethane, *iso*-butane), *iso*-butene and organic acids (formic and acetic) in classic- and photo-Fenton systems [14]; TBF, formaldehyde, and 2-methyl-propanal from both photolysis of methyl nitrite and Cl$^\bullet$ initiated atmospheric oxidation of MTBE [7]; TBF, formaldehyde, methyl acetate, and acetone from photolysis of ethyl nitrite [9]; TBF, methyl acetate, acetone, and TBA via ozone-sonolysis [25]. Idriss et al. [10] claimed methanol as a minor product in the atmospheric photocatalyzed oxidation of MTBE on fly ash. Trace amounts of *iso*-butene were found in the photocatalytic transformation of TBA in oxygenated TiO_2 slurries but not in that of MTBE [17]. Stefan et al. [20] found TBF, 2-methoxy-2-methyl propionaldehyde (MMP), formaldehyde, acetone, TBA, methyl acetate, hydroxy-*iso*-butyraldehyde, hydroxyacetone, pyruvaldehyde, and organic acids (hydroxy-*iso*-butyric, formic, pyruvic, acetic, oxalic) in MTBE oxidation in the UV–H_2O_2 system. Obviously, the products from the oxidation of MTBE are very similar when comparing various Fenton systems with other AOPs and the atmospheric NO_x–air system. All these reactions involve oxidation initiated by $^\bullet$OH. However, the quantity of each degradation product and the degradation pathways should be different due to the different features of the $^\bullet$OH generating systems. In addition to the $^\bullet$OH initiated free radical reactions, Fe^{2+} and Fe^{3+} may participate in the redox reactions and interact with the degradation intermediates in the Fenton system [30], which in turn will likely significantly impact the treatment efficiency and the product distribution. There is still a lack of reporting in the literature on the reactions between iron ions and MTBE degradation intermediates and on the roles of these reactions among the complex of free radical reactions and aqueous iron organometallic reactions for both AFT and CFT.

The goals of this study were (i) to determine the effectiveness of the anodic Fenton treatment systems in the remediation of MTBE, (ii) to optimize the hydrogen peroxide to iron ratios in the anodic Fenton treatment system for MTBE degradation, (iii) to investigate major degradation products formed during

the treatments, and (iv) to propose reaction mechanisms to shed more light on the roles of iron-ions among the complex of free radical reactions and aqueous iron organometallic reactions in both AFT and CFT. The combination of Fenton chemistry with MTBE degradation mechanisms in AFT will help build a kinetic model for further MTBE treatment at a larger scale.

2. Materials and methods

2.1. Chemicals

MTBE (99.9%), acetone (99.7%), methyl acetate (99.5%), TBA, ethyl acetate (99.9%), sodium chloride (analytical grade), ferrous sulfate heptahydrate, and ammonium bicarbonate were obtained from Fisher Scientific. TBF (99%) formic acid (96%), and ethanol (99.5%) were purchased from Aldrich (Milwaukee, WI) and methanol (HPLC grade) from Mallinckrodt (Paris, KY). Acetic acid (99.7%) was purchased from EM Scientific (Gibbstown, NJ).

2.2. Reaction apparatus and procedures

All experiments were conducted at ambient temperature (22–24 °C). For all treatments 100 mL of MTBE solution was used and kept agitated by a magnetic stir bar. The classic Fenton treatment (CFT) of aqueous MTBE was conducted in a 150 mL self-made air-tight pyrex glass apparatus. As presented below, the evaporative loss of MTBE from the aqueous solution was significant if the headspace of the apparatus was open to the air. During the reaction, reagents were added to the system by a peristaltic pump and aliquots were removed by syringe through a septum. The inlet and outlet of a small gas pump (about 4 W) were connected to the headspace of the apparatus to circulate the headspace gases through a 2.5 cm inner-diameter column packed with NaOH pellets to remove CO_2 from the headspace. The gas pump was assembled from a mini-vacuum (Jameco Electronic Components and Computer Products, Beltmont, CA) and was sealed air-tight. The purpose of removing CO_2 from the headspace was to accelerate the transfer of dissolved CO_2 from the solution to the headspace, which, from a chemical equilibrium and kinetics point of view, reduces its concentration in solution and consequently prevents suppression of MTBE mineralization by the CO_2 produced in the treatment. Tests confirmed that concentrations of MTBE and its volatile organic degradation products in aqueous solution were not changed significantly when the solutions were stirred in this apparatus for one hour, the maximum time for the treatments. The gas/water partition coefficients of the organic acids produced in the treatment [45] are so small that their loss through gas phase would be negligible (<3% in 64 min). The non-acidic MTBE degradation products were not found to decrease in 60 min in this system in the control experiments without any Fenton reagent (data not shown); to explain this, more experiments would need to be conducted, which is beyond the scope of this work. Anodic Fenton treatment (AFT) used a half-cell technology developed in this laboratory and described by Saltmiras and Lemley [36]. The anode was made from cold rolled steel plates immersed

in the aqueous MTBE solution. Current was delivered to the solution by changing the output current from a direct-current power source (DC Power Supply 1610, BC Precision Dynascan Co., Chicago, IL). The delivery rate for ferrous iron was 0 (0 A) to 0.075 mmol/min (0.24 A), verified by spectrometric analysis (vide infra). The cathodic cell (containing a bundle of graphite bars) and the anodic cell (also air-tight) were connected by a salt bridge filled with saturated sodium chloride solution. The cathodic half-cell was filled with the same solution as the salt bridge to slow down the diffusion of sodium chloride from the salt bridge. For all AFT experiments, aqueous H_2O_2 solution was added to the anodic half-cell by a peristaltic pump (Fisher Scientific, Pittsburgh, PA) at a flow rate of 0.5 mL/min. H_2O_2 concentrations of 0.25%, 1.3%, and 2.5% were used with a ferrous iron delivery rate of 0.037 mmol/min to obtain Fe^{2+}:H_2O_2 molar ratios of 1:1, 1:5, and 1:10. For CFT experiments, H_2O_2 (1.27% in water) and ferrous sulfate (0.23 M in water) solutions were pumped into the MTBE solution during the course of the treatment.

A 1.0 mL aliquot of the MTBE solution was removed by syringe at 1, 2, 4, 8, 16 and 32 min intervals during the treatment and added to a vial containing aqueous hydroxyl amine hydrogen chloride used for quenching •OH.

2.3. Sample preparation for treatment and analysis

Aqueous MTBE solution was prepared by dissolving MTBE into deionized water that was saturated with air. It was necessary to remove the dissolved iron from the samples to prevent iron-catalyzed degradation from occurring during the gas chromatographic (GC) analysis. Iron salts were precipitated when 2 M ammonium sulfide aqueous solution was added (20 μL for each milliliter of the treated solutions). Aqueous ammonia solution (10%, less than 5 μL for each milliliter of the treated solutions) or hexanoic acid aqueous solution (1 M, less than 5 μL for each milliliter of the treated solution) was added if necessary to adjust the pH to around 7. The samples were subsequently filtered through a 0.2 μm Nylon syringe filter (Alltech, Deerfield, IL) and then analyzed by a GC–mass spectrometer (MS).

2.4. GC–MS operating conditions

MTBE and its degradation products were analyzed on a Hewlett-Packard (Sunnyvale, CA) GC 5890 Series II coupled to a HP 5971A MS. Operating conditions and other aspects of the method were detailed in Ref. [46].

2.5. Analysis of iron ions

One package of ferrous ion reagents (Hach Co., Loveland, CO) containing 10-phenanthroline sodium bicarbonate was added to each 25 mL sample. The concentration of ferrous iron was quantified by measuring the absorbance at 510 nm. FerroVer Iron Reagent (Hach Co.) was used for the analysis of total iron ions. The quantity of ferric ion was the difference between total iron and the amount of ferrous ion.

2.6. Analysis of hydrogen peroxide

The concentration of hydrogen peroxide used for the Fenton reaction was determined by titration with $KMnO_4$ [47].

3. Results and discussion

3.1. Effects of ferrous salt and hydrogen peroxide on MTBE degradation

Control experiments were conducted to evaluate the effect of evaporation during treatment and to assess the stability of MTBE in acid solution. Preliminary experiments showed that the evaporative loss of MTBE from a 2.3 mM aqueous solution was about 40% and 60% at 8 min and 32 min, respectively (see Fig. S1 in Supporting Information), when the system was open to air while keeping the other experimental conditions the same as for CFT and AFT experiments, but with no reagents added. The evaporative loss of MTBE was negligible when the apparatus was air-tight, and thus the following experiments were all performed in this manner. No significant change in MTBE concentration (3 mM) was observed for 64 min under acidic conditions (pH 2.5).

Another control was conducted with ferrous sulfate reagent only. MTBE (3 mM) was mixed with 24 mM of ferrous sulfate in the CFT apparatus at pH 2.6. No change in the MTBE concentration was observed for 64 min, and the amount of ferrous ion oxidized to ferric ion (brown color) was negligible since visibly the solution remained colorless. This agrees with previous work showing that oxidation of ferrous ion to ferric ion by oxygen gas is very slow in aqueous solution (reaction rate less than 10^{-5} min^{-1} at pH values between 2 and 4) [48].

MTBE was further degraded in the presence of H_2O_2 but without iron in the system (Fig. S2 in the Supporting Information). Fifty-seven percent of MTBE remained after 32 min. The primary degradation intermediate was TBF. In addition, TBA, acetone and methyl acetate were relatively minor degradation products. The pH of the solution stayed at 6.5 during the process.
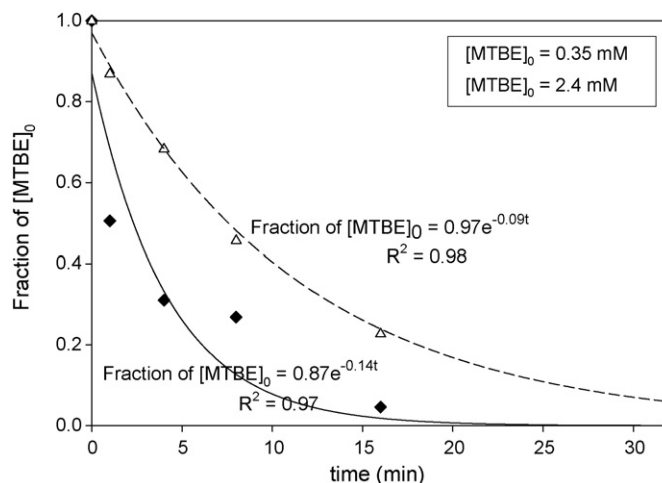

Fig. 1. Pseudo-first order fitting of MTBE degradation in AFT (Fe^{2+}:H_2O_2 = 1:1). Fe^{2+} and H_2O_2 were both added at 0.037 mmol/min by electrolyzing the iron anode and by pumping, respectively.

3.2. Kinetic degradation of MTBE in AFT and CFT

A typical degradation pattern of MTBE in either AFT or CFT is shown in Fig. 1, where the degradation kinetics can be approximated as pseudo-first-order. A series of experiments were conducted at different MTBE initial concentrations and Fe^{2+}:H_2O_2 ratios in either AFT or CFT (gradual or batch); the kinetics results are shown in Table 1. As can be seen from Table 1, complete degradation of MTBE was detected between 4 and 8 min for AFT at Fe^{2+}:H_2O_2 = 1:5 and for CFT-gradual with two different MTBE initial concentrations. Longer time (>16 min) was needed to degrade MTBE in AFT at other reagent ratios (1:1 or 1:10). In addition, as shown in Table 1, the pseudo-first-order degradation rate constant for AFT treatment increased as the molar ratio of Fe^{2+}:H_2O_2 changed in the following order: 1:0 < 1:1 < 1:10 < 1:5, suggesting that the optimum Fe^{2+}:H_2O_2 ratio is 1:5 in MTBE treatment. At this optimized Fe^{2+}:H_2O_2 ratio, CFT-gradual was found to behave similarly to AFT in

Table 1
Degradation kinetics of MTBE in AFT and CFT under different reaction conditions

[MTBE]$_0$ (mM)	Treatment device	Fe^{2+}:H_2O_2	k_{1st}[a]	R^2[b]	Time[c] (min)
3	AFT	1:0	0.02	0.87	>32
3.5	AFT	1:10	0.19	0.95	16
3.7	AFT	1:5	0.56	0.99	8
0.89	AFT	1:5	1.24	0.99	4
0.73	AFT	1:5	1.54	0.96	4
2.4	AFT	1:1	0.09	0.98	>32
0.35	AFT	1:1	0.14	0.97	32
2.8	CFT-gradual[d]	1:5	0.77	0.98	8
4.5	CFT-gradual[d]	1:5	0.53	0.99	8
1.8, 2.8, 3.6	CFT-batch[e]	1:5	>1.6	N/A[f]	1

[a] Pseudo-first-order rate constant (min^{-1}).
[b] Square of semi-log regression correlation coefficients.
[c] Time (min) when MTBE was completely degraded.
[d] CFT with Fe^{2+} and H_2O_2 added gradually during the course of treatment.
[e] CFT with Fe^{2+} and H_2O_2 added at the beginning of treatment.
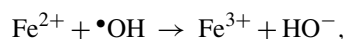[f] Reaction rate was too fast to be measured for an exact value.

terms of the reaction rate constant, while CFT-batch degraded MTBE much faster (Table 1) (see discussion at the end of Section 3.3).

The maximum degradation rate at the ratio of 1:5 in AFT experiments with similar MTBE initial concentrations suggests that the $^{\bullet}OH$ concentration generated by the Fenton reaction (reaction (1)) at this ratio was at the maximum level to react with MTBE (reaction (2)). Excess H_2O_2 was required beyond the stoichiometric amount needed for the Fenton reaction for a faster degradation of MTBE. These results can be explained by the regeneration of Fe^{2+} in the system which in turn could affect the actual Fe^{2+}:H_2O_2 ratio. While reaction (6) may be too slow to have much effect,
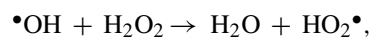
$$Fe^{3+} + H_2O_2 \rightarrow Fe^{2+} + HO_2^{\bullet},$$
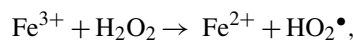
$$k_6 = 0.01\text{--}0.02\,M^{-1}\,s^{-1}\ [49] \tag{6}$$

other organic radicals generated in the reaction system could transfer electrons to Fe^{3+} to regenerate Fe^{2+} as discussed further in Section 3.5. At ratios greater or less than 1:5, excess Fe^{2+} or H_2O_2 can quench $^{\bullet}OH$ (reactions (7) and (8)), causing slower degradation of MTBE:

$$Fe^{2+} + {}^{\bullet}OH \rightarrow Fe^{3+} + HO^{-},$$

$$k_7 = 4.3 \times 10^8\,M^{-1}\,s^{-1}\ [22] \tag{7}$$

$${}^{\bullet}OH + H_2O_2 \rightarrow H_2O + HO_2^{\bullet},$$

$$k_8 = 2.7 \times 10^7\,M^{-1}\,s^{-1}\ [22] \tag{8}$$

In several sets of experiments (Table 1, Fig. 1), the initial concentration of MTBE ([MTBE]$_0$) was varied from 0.35 to 3.7 mM to determine its effect on the degradation kinetics. While keeping other conditions constant, a higher initial concentration of MTBE corresponded to a slower degradation (e.g., at Fe^{2+}:$H_2O_2 = 1$:5, the pseudo-first order rate constant k_{1st} was 0.56, 1.24, and 1.54 min^{-1} when [MTBE]$_0$ was 3.7, 0.89, and 0.73 mM, respectively), most probably due to the generation of a larger concentration of degradation intermediates (reaction (2)), which would consume $^{\bullet}OH$ (reaction (3)) and hence decrease the pseudo-first order rate constant of the parent compound. For comparison, first-order rate constants in the range of 4.1×10^{-4} to $8.5 \times 10^{-4}\,s^{-1}$ for MTBE degradation ([MTBE]$_0 = 1.0$–0.01 mM) were observed in ozone-sonolysis treatment [13], and from 7.1 to 0.18 min^{-1} ([MTBE]$_0 = 0.08$–85 mg L^{-1}) for MTBE degradation by the UV/H_2O_2 process [20].

3.3. MTBE degradation products in AFT and CFT

MTBE degradation products were detected in AFT experiments at two different Fe^{2+}:H_2O_2 ratios of 1:5 and 1:10. Regardless of the reagent ratio, acetone, TBF, TBA, acetic acid and formic acid were found to be the common products, while methyl acetate was not detected (Figs. 2 and S3 in the Supporting Information). The experimental errors on measured concentrations are less than 4% for MTBE, acetone, and TBF; less than 6% for TBA; and less than 9% for formic acid and acetic
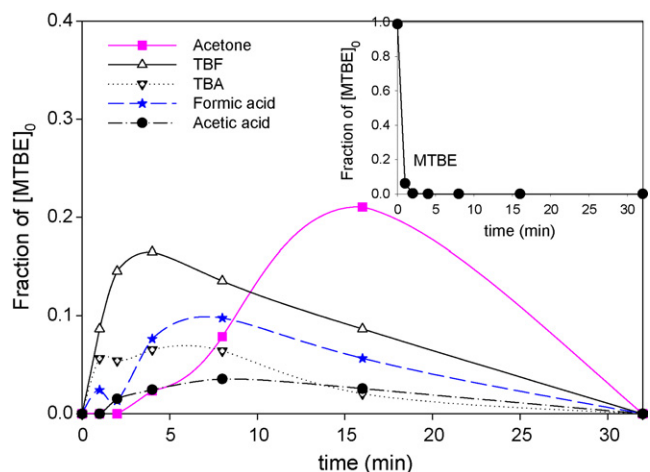

Fig. 2. Evolution of MTBE (shown in the insert) and its degradation products in AFT ([MTBE]$_0 = 0.89$ mM, Fe^{2+}:$H_2O_2 = 1$:5), Fe^{2+} and H_2O_2 were added at 0.037 and 0.19 mmol/min, respectively.

acid. Note that acetone appeared later and reached the highest concentration among all products. Generally, the maximum concentrations of the degradation products are in the order: acetone > TBF > formic acid > TBA > acetic acid at the Fe^{2+}:H_2O_2 ratio of 1:5 and in the order: acetone ≈ TBF > TBA > formic acid ≈ acetic acid at the Fe^{2+}:H_2O_2 ratio of 1:10. A smaller amount of formic acid was observed when the Fe^{2+}:H_2O_2 ratio was decreased from 1:5 to 1:10. In addition, both MTBE and its reaction products decreased more slowly at the lower Fe^{2+}:H_2O_2 ratio (1:10 versus 1:5) (Figs. 2 and S3).

A similar product profile was also observed for the degradation of MTBE ([MTBE]$_0 = 2.8$ or 4.5 mM) in CFT with a gradual delivery of Fe^{2+} and H_2O_2 (see Fig. S4 in the Supporting Information). The degradation products detected were acetone, TBF, TBA, and methyl acetate. Acetic acid and formic acid were not analyzed in these experiments. The maximum concentration of the degradation products are in the order: acetone > TBF > TBA > methyl acetate (trace amount).

In CFT-batch experiments (Fig. S5 in the Supporting Information), MTBE completely degraded within one min. However, all degradation products were still present at a significant amount after 32 min of treatment. The degradation products detected were acetone, TBF, TBA, acetic acid, formic acid, and methyl acetate. As in all other types of treatment, acetone was the most abundant degradation product, followed by TBF ≈ acetic acid > TBA ≈ methyl acetate > formic acid. No methanol was detected. Acetaldehyde was present at a low level (<0.02 mM) in some of the CFT-batch treatments (data not shown) (see Ref. [20] for the reaction mechanism). No acetaldehyde or methanol was detected for either AFT or CFT-gradual treatment of MTBE. Acetic acid and formic acid were observed in amounts greater than 0.017 mM (~5% of [MTBE]$_0$) for most of the above treatments. Similar to the case of AFT, acetic acid was more abundant than formic acid in treatments with higher concentrations of H_2O_2 (CFT-batch and 1:10 AFT versus 1:5 AFT).

A high concentration of carbon dioxide was observed for all Fenton treatments, based on GC–MS analysis. However, the GC–MS analysis of carbon dioxide was significantly

affected by the chemical composition of the sample and is only semi-quantitative. For these reasons, carbon dioxide was not quantified in the MTBE treatment.

Three break-down products – TBF, TBA, and methyl acetate – decayed faster in the CFT-gradual treatment than in the CFT-batch treatment. This result is interesting because the degradation of MTBE itself was much faster in CFT-batch than in any other treatment. Based on reaction (1), addition of both Fenton reagents (Fe^{2+} and H_2O_2) at once at the beginning of the CFT-batch is believed to result in a higher initial concentration of $^{\bullet}OH$ compared to the other treatment methods As shown in reactions (7) and (8), $^{\bullet}OH$ immediately reacted with the surrounding Fe^{2+} and H_2O_2 as well as with itself and MTBE, due to its high and non-selective reactivity [29]. This explains why there was a larger amount of degradation products remaining at the end (32 min) of the CFT-batch experiment than that of AFT.

3.4. Detectable total organic carbon remaining (DTOC) after MTBE degradation in AFT and CFT

Fig. 3 shows the time course of detectable total organic carbon remaining (DTOC) for each treatment. DTOC was calculated by adding up the fractions of all the organic compounds detected at a certain treatment time (up to 32 min) on the basis of the carbon molarity each compound contains. Note that the experimental error for DTOC is 0.05. During the initial 4 min of treatment, AFT at Fe^{2+}:H_2O_2 ratio of 1:5 had the fastest decay of DTOC, followed by CFT-batch, CFT-gradual, and then AFT treatments not at the optimum Fe^{2+}:H_2O_2 ratio (i.e., 1:1 and 1:10). After the initial stage, DTOC decayed slowly and reached 0.14 at 32 min for CFT-batch, reached zero for CFT-gradual and AFT at Fe^{2+}:H_2O_2 ratio of 1:5, and decayed more slowly for AFT

at other Fe^{2+}:H_2O_2 ratios. DTOC in the MTBE treatment with H_2O_2 alone was still 0.71 after 32 min of treatment. Thus the Fenton reaction at any Fe^{2+}:H_2O_2 ratio was much more efficient than H_2O_2 alone for the treatment of MTBE in water. The highest DTOC degradation efficiency in AFT at the Fe^{2+}:H_2O_2 ratio of 1:5 also supports the previous conclusion that Fe^{2+} is regenerated in the Fenton system to consume H_2O_2 beyond the stoichiometric demand (see reaction (1)), and that too much Fe^{2+} and H_2O_2 will quench $^{\bullet}OH$ through reactions (7) and (8). The effect of the MTBE initial concentration is shown in Fig. 3b; DTOC was found to decay more slowly at a higher MTBE concentration if other conditions remained the same, clearly due to the presence of a larger amount of compounds (MTBE and its intermediates) that react with $^{\bullet}OH$.

3.5. Mechanisms for MTBE degradation via anodic Fenton reaction

The degradation of MTBE and its breakdown products by anodic Fenton reaction involves numerous reactions among free radicals, neutral compounds, oxygen, organic ions, and ferrous and ferric ions. The involvement of the iron ions makes it more complicated than the free radical degradation pathways that have been reported [7–10,13–29]. Our discussion of the mechanisms focuses on the uncharted redox reactions that involve iron ions and related free radicals as well as the radical α and β scissions.

3.5.1. Generation of primary intermediates (Schemes 1 and 2)

As stated earlier, the presence of Fe^{2+} and Fe^{3+} ions makes the degradation of MTBE in the Fenton system more complex than that proposed for the UV/H_2O_2 system. Walling [30]
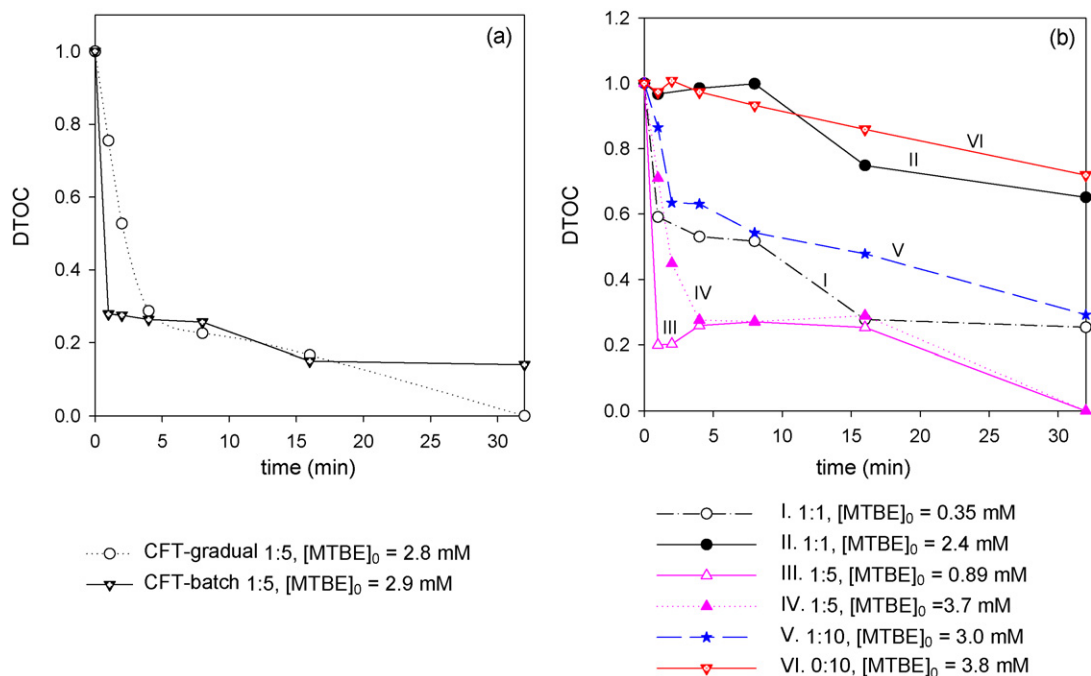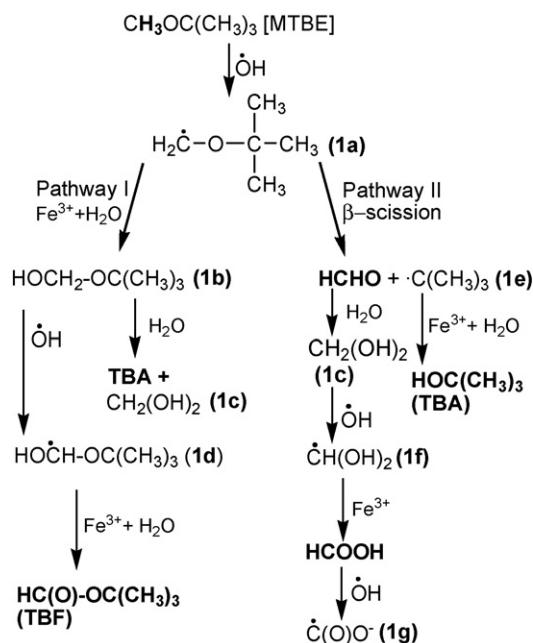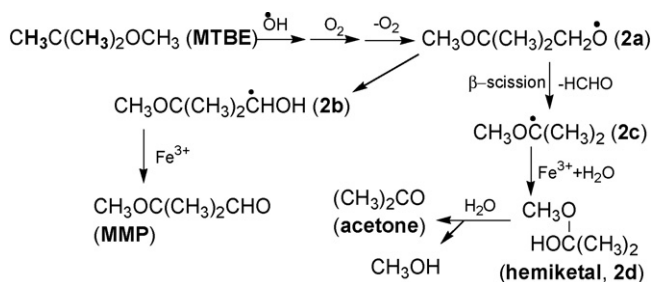

Fig. 3. Evolution of DTOC (detectable total organic carbon remaining) in MTBE degradation in (a) CFT and (b) AFT at different Fe^{2+}:H_2O_2 ratios with different MTBE initial concentrations.

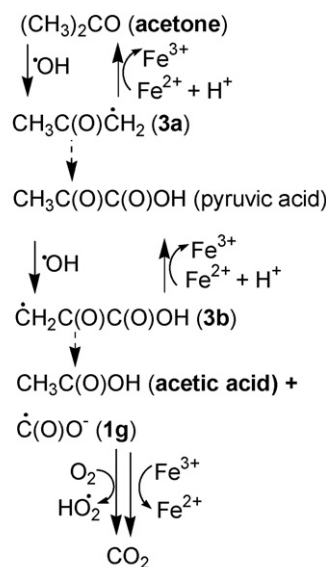Scheme 1. Fe^{3+}/Fe^{2+} participating degradation of MTBE initiated by $^{\bullet}OH$ H-abstraction from methoxyl group.

Note: A dashed arrow denotes multiple steps involved.

Scheme 3. Fe^{3+}/Fe^{2+} participating degradation of acetone.

reported that C-centered organic radicals containing α-OH or α-OR (typical electron-donating groups) can reduce Fe^{3+} rapidly to Fe^{2+} with the rate constant estimated to be $>4 \times 10^8 \, M^{-1} \, s^{-1}$ for $^{\bullet}CH_2OH$, while primary and secondary alkyl radicals are inert toward such reactions. In the Fenton treatment of MTBE, the $^{\bullet}OH$ extracts hydrogen from the methoxy group of MTBE, resulting in the C-centered radical **1a** (Scheme 1). In addition to reacting with O_2, **1a** also reacts with Fe^{3+}, forming intermediate **1b** via pathway I in Scheme 1. Hydrolysis of **1b** yields TBA and **1c**. The $^{\bullet}OH$ H-abstraction from **1b** generates the C-centered radical **1d** (pathway I in Scheme 1). Radical **1d** should be potently reductive [30] and can be oxidized by Fe^{3+} to TBF. In pathway II, β-scission occurs in radical **1a**, producing formaldehyde and the C-centered *t*-butyl radical **1e**; **1e** is then oxidized by Fe^{3+} to form TBA.

The $^{\bullet}OH$ also extracts hydrogen from the *t*-butoxy side of MTBE producing a C-centered radical; this radical reacts with O_2 to form a peroxyl radical; two peroxyl radicals dimerize to form a tetraoxide, which cleaves into two oxy radicals, **2a**, and one O_2 (Scheme 2). The α-hydrogen can rapidly shift to the oxygen [59], converting **2a** to the C-centered radical

Scheme 2. Fe^{3+}/Fe^{2+} participating degradation of MTBE initiated by $^{\bullet}OH$ H-abstraction from butoxyl group.

2b. **2b** is potently reductive [30] and is oxidized by Fe^{3+} to $CH_3OC(CH_3)_2CHO$ (MMP). A β-scission can also occur in **2a** and release formaldehyde and a reductive C-centered radical **2c**, which is oxidized by Fe^{3+} to the hemiketal **2d**. **2d** is hydrolyzed to acetone and methanol (Scheme 2). Since methanol was not detected in our experiments, this β-scission should be a minor route of the pathways.

3.5.2. Degradation of primary intermediates

Reaction rate constants and major degradation products of the primary intermediates – acetone, TBF, TBA, acetic acid, formic acid, HCHO, and MMP – by reaction with $^{\bullet}OH$ are shown in Table 2. Detailed oxidation mechanisms of the primary intermediates by $^{\bullet}OH$ have been reported [20,51,52]. Not all reaction products were analyzed in this study. Because $^{\bullet}OH$ is the primary oxidant in the Fenton system, the authors expect that the same products as shown in Table 2 should also exist in AFT and CFT treatment of MTBE, but additional reactions should occur due to the presence of ferric and ferrous ions.

Acetone is the most abundant oxidation product under various reaction conditions. It is not only a reaction intermediate of MTBE, but also an intermediate in the oxidation of TBF, TBA and MMP (Table 2), which explains its continuous accumulation in AFT and CFT until all other compounds have been consumed (Fig. 2 and Figs. S3–S5). The high abundance of acetone is also related to its relatively lower oxidation rate with $^{\bullet}OH$ (Table 2). As reported by Stefan et al. [51,52], oxidation of acetone by $^{\bullet}OH$ is initiated by H-abstraction at one of the methyl groups and continued by free radical reactions forming various products, with oxalic acid, acetic acid, and formic acid as the predominant ones (Table 2). Fe^{3+} is not expected to react with the formed acetone radical ($CH_3COCH_2^{\bullet}$, **3a** in Scheme 3) to any appreciable extent due to the existence of the electron-withdrawing carbonyl group [30]. **3a** is transferred to pyruvic

Table 2
Reaction rate constants and oxidation products of MTBE and its degradation intermediates with hydroxyl radicals

Chemical	$k_{\bullet OH}$ (M^{-1} s^{-1})	Primary oxidation products	References
MTBE	1.6×10^{9}[a]	Acetone, HCHO, formic acid, acetic acid, TBF, TBA, MMP, methyl acetate	[20]
HCHO	1.0×10^{9}[b]	Formic acid	[51,52]
Acetone	1.1×10^{8}[b]	Acetic acid, formic acid, HOOCCOOH	[51,52]
TBF	4.1×10^{8}[c]	Acetone, HCHO, formic acid, HOC(CH$_3$)$_2$CHO, HOC(CH$_3$)$_2$COOH, CH$_3$COCOOH	[20]
TBA	6×10^{8}[b]	Acetone, HCHO, HOC(CH$_3$)$_2$CHO, HOC(CH$_3$)$_2$COOH	[20]
Formic acid	1.3×10^{8}[b]	CO$_2$	[51,52]
Acetic acid	1.6×10^{7}[b]	HOOCCOOH, formic acid	[51,52]
Methyl acetate	1.2×10^{8}[b]	Acetic acid, formic acid	This paper
MMP	NA	Acetone, HCHO, formic acid, CO$_2$, HOC(CH$_3$)$_2$COOH, CH$_3$COCOOH	[20]

[a] Ref. [31].
[b] Ref. [29].
[c] Ref. [61].

acid through several free radical reactions already described in the literature [51]. It is of interest that **3a** and the subsequently formed radical **3b** can be reduced by Fe^{2+} in the presence of the carbonyl group with a reaction rate constant $>10^7$ M^{-1} s^{-1} [30] (Scheme 3). As reported earlier [53], Fe^{3+} was the dominant iron species in the AFT system. Thus, such reduction by Fe^{2+} may be a minor pathway in acetone degradation.

TBF is the second most abundant MTBE oxidation intermediate. It is mainly formed through pathway I in Scheme 1. Its relatively large $k_{\bullet OH}$ and fast accumulation during the initial stage of MTBE degradation (Fig. 2 and Figs. S3–S5) indicate the importance of pathway I in the overall reaction of MTBE (Scheme 1). For TBF degradation mechanisms there are two possible sites for $\bullet$OH H-abstraction. It is believed that the attack at the formyl group (forming radical **4b** in Scheme 4) is more likely than at the three methyl groups (forming radical **4a** in Scheme 4) because $\bullet$OH is electrophilic [20]. In addition to combining with O$_2$ into the peroxide radical routes, radical **4b** is likely to undergo α- or β-scission because the bonds in radicals are weakened compared to the non-radical molecules [54]. The α-scission dominates over the β-scission for radical **4b** because the unpaired electron is located on the carbon of the carbonyl group [54]. Fe^{3+} can then oxidize (CH$_3$)$_3$C$^{\bullet}$ (**1e** in Schemes 1 and 4), forming TBA (Scheme 4) [30].

TBA is generated from MTBE both through Scheme 1 and from TBF (Scheme 4). Its abundance is generally right below that of TBF (Figs. S3–S5), except in two cases where the abundance of either acetic acid or formic acid is in between (see more discussion below). Considering the similar reaction rate constants of TBF and TBA, the lower abundance of TBA than that of TBF confirms that pathway I in Scheme 1 – leading to the generation of both TBF and TBA – is more important than pathway II in Scheme 1—leading to the generation of TBA only.

The attack of the $\bullet$OH on TBA occurs at one of the methyl groups [55]. Most of the C-centered radicals formed will combine with oxygen to form a tetraoxide, which will eventually lead to the generation of products in Table 2 (for detailed mechanism see Refs. [7,20]). The oxy radical **4e** in Scheme 4 is generated in this process. **4e** cleaves to formaldehyde HCHO and radical **4f**, which is then oxidized to acetone by Fe^{3+} (Scheme 4).

Formaldehyde is a common product for MTBE and its degradation intermediates (Schemes 1 and 4, Table 2). It quickly hydrates to CH$_2$(OH)$_2$ (**1c**) [56] in the gas phase containing water vapor [56] and thus should occur even more quickly in the aqueous phase with a higher water concentration. **1c** is further transformed via $\bullet$OH H-abstraction to the C-centered radical **1f**, which is then oxidized by Fe^{3+} to formic acid, another common product for MTBE and its intermediates (Table 2). HCOOH is converted to radical **1g** through $\bullet$OH H-abstraction (Scheme 1). The reductive radical **1g** (pK_a = 1.4) is also formed from acetone degradation (Scheme 3) and can be rapidly oxidized to CO$_2$ by Fe^{3+} and O$_2$ (Scheme 3) [56,30]. It is not clear why a higher percentage of formic acid is formed in AFT at the optimum Fe^{2+}:H$_2$O$_2$ ratio than under other conditions (Fig. 2 versus Figs. S3 and S4), but more formic acid generation indicates a better capacity to mineralize MTBE because formic acid is believed to react with the $\bullet$OH radical leading to CO$_2$ production—the final mineralization of the system (Table 2) [20].

Acetic acid is reported to be the degradation product of acetone and methyl acetate (Table 2). Oxidation of TBF, TBA, and MMP indirectly generates acetone and hence acetic acid. The oxidation rate of acetic acid (1.6×10^7 M^{-1} s^{-1}) is about one-order of magnitude slower compared to that of MTBE and its
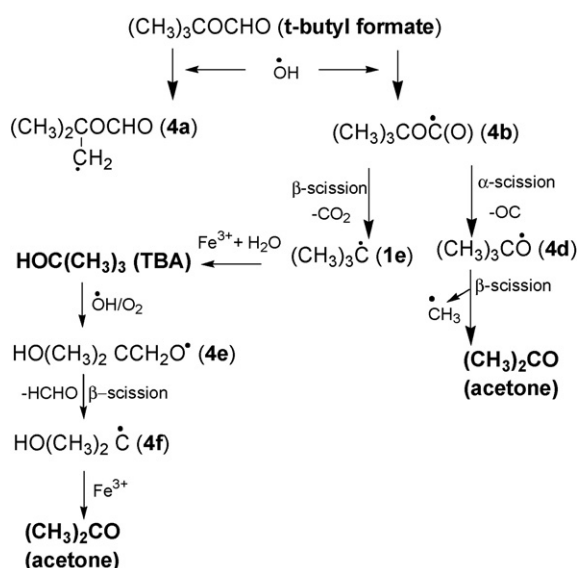
Scheme 4. Degradation of *t*-butyl formate and *t*-butyl alcohohl.

oxidation intermediates ($>1.1 \times 10^8$ M^{-1} s^{-1}) (Table 2). Stefan et al. [20] reported a high production of acetic acid in MTBE degradation in the UV/H$_2$O$_2$ process and attributed it to various sources during treatment. Its high concentration in CFT-batch supports the above conclusion. However, its maximum concentration was the lowest among the detected MTBE oxidation intermediates in AFT treatments (Figs. 2 and S3), likely due to the higher treatment efficiency of AFT compared to that of CFT-batch. In other words, acetic acid further degraded in AFT. Acetic acid is reported by others to form oxalic acid and formic acid as the final oxidation products by $^\bullet$OH [20].

Pathways for methyl acetate generation are not important because methyl acetate was not detected in AFT systems (Figs. 2 and S3), but may be generated at a concentration below the detection limit (i.e., 0.01 μg/ml) [24,26], and very low production of methyl acetate was found in CFT systems (Figs. S4 and S5). The $^\bullet$OH-initiated radical degradation mechanisms of MMP and methyl acetate were already studied [7,20], and thus are not discussed in this paper.

3.5.3. Generic degradation scheme for MTBE and its oxidation intermediates in a Fenton system

On the basis of our experimental results and literature reports [7–10,13–30,51,52], Scheme 5 summarizes the generic pathways that MTBE and its break-down products follow in an anodic or classic Fenton system. The degradation of MTBE or its break-down product **5a** is initiated by H-abstraction from carbon by $^\bullet$OH generated in the Fenton reaction to form radical **5b** with a rate constant between 10^6 and 10^9 M^{-1} s^{-1} [29] (pathway a). Since $^\bullet$OH is electrophilic, its reactivity for abstraction of hydrogen from the carbons of **5a** is enhanced by electron-donating group(s) on the carbons following the order: α-OR (R is alkyl group or H) >α-R and is reduced by electron-withdrawing groups such as the α-carbonyl group in acetone and acetic acid [30]. Dimerization of radical **5b** should be negligible because

the concentration of **5b** is low (less than 4 mM) [50], and no dimers were detected in our experiments. H-abstraction by $^\bullet$OH from the hydroxyl group of intermediates such as TBA is negligible [55,58]. Furthermore, H-abstraction from MTBE and its break-down products **5a** by oxy radicals **5h** or peroxyl radicals **5c** is negligible because the reactivity should be 3–5 orders less than that by $^\bullet$OH [54].

Depending on its structure, radical **5b** can undergo degradation via five different pathways. In pathway b, α/β-scission occurs forming radicals and non-radical products. In pathway c, radical **5b** combines with oxygen to form a peroxyl radical **5c**, which can generate **5d** if substitutent A = OH (pathway g), or dimerize to form a tetraoxide **5f** (pathway h), or be reduced by Fe^{2+} to form an oxy radical **5g** (pathway i). Following pathway h, if substitutent A = H (such as in the methoxy group of MTBE), **5f** can either lose an oxygen, generating **5d** and **5e** (pathway j), or lose an H$_2$O$_2$, generating two **5d** products (pathway k). In addition, **5f** will lose dioxygen forming an oxy radical **5g** (pathway l). Three possible reactions can occur for radical **5g**: pathway m—1,2-H shift leading to radical **5h** if substitutent A = H; pathway n—α/β-scission; and pathway o—disproportionation to form **5d** and **5e**. In addition to pathways b and c, radical **5b** (and radical **5h**) can be oxidized by Fe^{3+} to either **5d** (pathway d, A = OH) or **5e** (pathway e, A = alkoxyl or alkyl), depending on the nature of substitutent A (examples have been discussed in the previous sections). Finally, in the presence of an electron-withdrawing substitutent, radical **5b** can be reduced to the parent compound **5a** by Fe^{2+} (pathway f) through an inner sphere mechanism with RO$_2$-Fe^{3+} as the intermediate [59,60].

Pathway c has reaction rate constants ranging from 10^7 to 10^9 M^{-1} s^{-1} [57], pathways d and e have rate constants $>4 \times 10^8$ M^{-1} s^{-1} [30], and pathway f has a rate constant $>10^7$ M^{-1} s^{-1} [30]. Since iron was continuously introduced into the 100 mL AFT system at 0.037 mmol/min and Fe^{3+} was reported to be the dominant iron species in the AFT system [53],
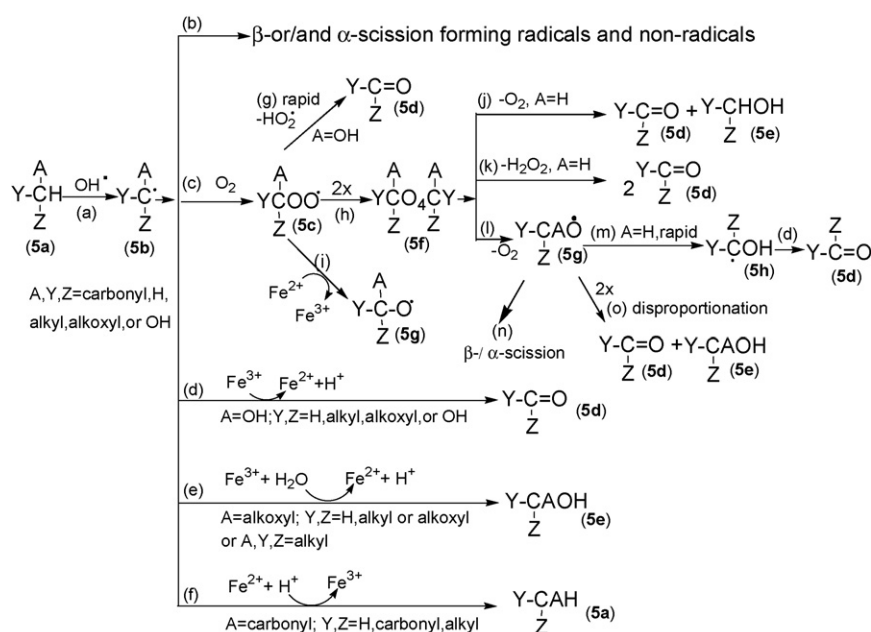
Scheme 5. General degradation mechanisms of MTBE and its oxidation products in a Fenton system.

the much higher concentration of Fe^{3+} (1–3 mM, data not shown) – compared to the concentration of dissolved O_2 (0.24 mM at saturation) – would make oxidation through pathways d and e preferable to O_2-addition (pathway c) over the entire course of the treatment.

In pathway c, the formation of peroxyl radicals **5c** from primary C-centered radicals and dissolved oxygen is irreversible and diffusion-controlled (2–$4 \times 10^9 \, M^{-1} \, s^{-1}$) [50]. For secondary peroxyl radicals, the rate constant is around $10^7 \, M^{-1} \, s^{-1}$. These fast reaction rates make this reaction limited only by the availability of the dissolved O_2. The dissolved O_2 can be consumed to a fairly low level by the C-centered radicals generated from the $^{\bullet}OH$ H-abstraction of MTBE (>0.5 mM initially) [51,52]. If O_2 concentration is low enough, the formation of peroxyl radical (**5c**) in pathway c could compete with either pathway b or pathway d/e. However, O_2 will not be depleted because there are several reactions that generate O_2 (e.g., pathways j and l). In fact, Xu and Gu [27] detected an increase in the concentration of dissolved oxygen over a long reaction period (>20 min) in the Fenton reaction, and attributed it to the reaction below:

$$^{\bullet}O_2H + Fe^{3+} \rightarrow O_2 + Fe^{2+} + H^+ \qquad (9)$$
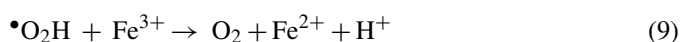
Note that $^{\bullet}O_2H$ is mainly generated via reaction (6).

In pathways d and e, the reductive reactivity of **5b** is estimated to decrease in the order of the electron donating ability of its substitutent groups: α-OH > α-OR > α-R > α-H > α-carbonyl. Fe^{2+} is regenerated via these pathways so that the optimum ratio of Fe^{2+}:H_2O_2 in AFT is 1:5 instead of the stoichiometric 1:1. Such a ratio also indicates that the reduction of **5b** by Fe^{2+} in pathway f is relatively insignificant, and that H_2O_2 is not generated to a scale comparable with the regeneration of Fe^{2+}. Therefore, pathway k that regenerates H_2O_2 is not expected to be significant.

Radical β-scission and α-scission in pathways b and n are likely to occur frequently during Fenton treatment of MTBE because bonds in radicals are weaker than those in non-radical molecules [54]. Furthermore, water accelerates the scission of radicals significantly compared to gas phase [58]. The formation of double bonds in the non-radical products (e.g., HCHO, acetone, CO_2, and CO) also contributes to the fast rates [54]. Similar to the fast β-scission of radical **4d** to form acetone as shown in Scheme 4 ($10^6 \, s^{-1}$) [59], many of the other radical β- and α-scissions in Schemes 1–5 should be rapid enough to compete with both the formation of peroxyl radical **5c** (pathway c) and redox reactions with Fe^{3+}/Fe^{2+} (pathways d–f) in Scheme 5.

4. Conclusions

This study has investigated the degradation of MTBE and its oxidation products in two Fenton systems (AFT and CFT). The optimum molar ratio of Fe^{2+}:H_2O_2 for AFT is 1:5. Gradual delivery of ferrous ion and H_2O_2 is more efficient than batch input of reagents to degrade MTBE and its break-down products using Fenton treatment, which warrants further study of AFT treatment of MTBE on a larger scale, namely, for both AFT and CFT, the continuous input of reagents is better than the batch input in regard to process efficiency. MTBE and its break-down products completely degraded in 32 min when ferrous ion and H_2O_2 were delivered into the treatment system via AFT at an Fe^{2+}:H_2O_2 ratio of 1:5. The degradation of MTBE was slower as the initial MTBE concentration increased. Similar to previous findings, the three most significant degradation products detected were acetone, TBF, and TBA, while acetic acid, formic acid, and methyl acetate were minor products. Other products such as MMP and HCHO, although not targeted in this study, could also be among the degradation products at a low level based on the work of others.

On the basis of the experimental results and the literature, the degradation mechanisms of MTBE and its breakdown products in AFT and CFT were proposed. Generally, reactions are initiated by H-abstraction by $^{\bullet}OH$ generating C-centered radicals, which undergo various reactions including α/β-scission within the radical, combination with oxygen, oxidation by ferric ions, and reduction by ferrous ions before generating the final oxidation products. The predominant pathways are believed to be radical combination with oxygen (and the reactions thereafter), radical oxidation by ferric ions, and α/β-scission within the radical. Radical reduction by ferrous ions is the least important pathway in the overall fate of the generated radicals. Overall, by understanding the reaction kinetics and mechanisms of MTBE degradation in the anodic Fenton system, this study offers a potential remediation technique for treating MTBE contaminated wastewater.

Acknowledgments

Appendix A. Supplementary data

Supplementary data associated with this article can be found, in the online version, at doi:10.1016/j.jhazmat.2006.12.030.

References

[1] American Petroleum Institutes Soil and Groundwater Technical Task Force, API Soil and Groundwater Research Bulletin 3, 1998.

[2] G.C. Delzer, J.S. Zogorski, T.J. Lopes, R.L. Bosshart, Water Resources Investigations Report 96-4145, USGeographical Survey, Denver, 1996.

[3] P.J. Squillace, J.F. Pankow, N.E. Korte, J.S. Zogorski, Review of the environmental behavior and fate of methyl *tert*-butyl ether, Environ. Toxicol. Chem. 16 (1997) 1836.

[4] P.J. Squillace, J.S. Zogorski, W.G. Wilber, C.V.J. Price, A preliminary assessment of the occurrence and possible sources of MTBE in groundwater in the United States, 1993–1994, Environ. Sci. Technol. 30 (1996) 1721.

[5] P.H. Howard, R.S. Boethling, W.M. Meylan, E.M. Michalenko, Handbook of Environmental Degradation Rates, Lewis Publishers, 1991.

[6] L. Zwank, M. Berg, M. Elsner, T.C. Schmidt, R.P. Schwarzenbach, S.B. Haderlein, New evaluation scheme for two-dimensional isotope analysis to decipher biodegradation processes: application to groundwater contamination by MTBE, Environ. Sci. Technol. 39 (2005) 1018–1029.

[7] S.M. Japar, T.J. Wallington, J.F.O. Richert, J.C. Ball, The atmospheric chemistry of oxygenated fuel additives: *tert*-butyl alcohol, dimethyl ether, and methyl *tert*-butyl ether, Int. J. Chem. Kinet. 22 (1990) 1257.

[8] D.F. Smith, T.E. Kleindienst, E.E. Hudgens, C.D. McIver, J.J. Bufalini, The photooxidation of methyl *tert*-butyl ether, Int. J. Chem. Kinet. 23 (1991) 907.

[9] E.C. Tuazon, W.P.L. Carter, S.M. Aschmann, R. Atkinson, Products of the gas-phase reaction of methyl *tert*-butyl ether with the OH radical in the presence of NO*x*, Int. J. Chem. Kinet. 23 (1991) 1003.

[10] H. Idriss, A. Miller, E.G. Seebauer, Photoreactions of ethanol and MTBE on metal oxide particles in the troposphere, Catal. Today 33 (1997) 215.

[11] R.J. Steffan, K. McClay, S. Vainberg, C.W. Condee, D. Zhang, Biodegradation of the gasoline oxygenates methyl *tert*-butyl ether, ethyl *tert*-butyl ether, and *tert*-amyl methyl ether by propane-oxidizing bacteria, Appl. Environ. Microb. 63 (1997) 4216.

[12] C.K. Yeh, J.T. Novak, Anaerobic biodegradation of gasoline oxygenates in soils, Water Environ. Res. 66 (1994) 744.

[13] J.W. Kang, M.R. Hoffmann, Sonolytic destruction of methyl *tert*-butyl ether by ultrasonic irradiation: the role of O_3, H_2O_2, frequency, and power density, Environ. Sci. Technol. 33 (1999) 3199.

[14] N. Charton, C. Guillard, C. Hoang-Van, P. Pichat, Products of MTBE degraded in water by the photo-Fenton reaction, PSI-Proc. 97-02 (1997) 65.

[15] J.L. Graham, R. Striebich, C.L. Patterson, E.R. Krishnan, R.C. Haught, MTBE oxidation byproducts from the treatment of surface waters by ozonation and UV-ozonation, Chemosphere 54 (2004) 1011–1016.

[16] M.M. Mitani, A.A. Keller, C.A. Bunton, R.G. Rinker, O.C. Sandall, Kinetics and products of reactions of MTBE with ozone and ozone/hydrogen peroxide in water, J. Hazard Mater. 89 (2002) 197–212.

[17] R.D. Barreto, A.G. Kimberly, A. Krista, Photocatalytic degradation of methyl-*tert*-butyl ether in TiO_2 slurries: a proposed reaction scheme, Water Res. 29 (1995) 1243.

[18] M. Bertelli, E. Selli, Kinetic analysis on the combined use of photocatalysis, H_2O_2 photolysis, and sonolysis in the degradation of methyl *tert*-butyl ether, Appl. Catal. B-Environ. 52 (2004) 205–212.

[19] E. Selli, C.L. Bianchi, C. Pirola, M. Bertelli, Degradation of methyl *tert*-butyl ether in water: effects of the combined use of sonolysis and photocatalysis, Ultrason. Sonochem. 12 (2005) 395–400.

[20] M.I. Stefan, J. Mack, J.R. Bolton, Degradation pathways during the treatment of methyl *tert*-butyl ether by the UV/H_2O_2 process, Environ. Sci. Technol. 34 (2000) 650.

[21] Y. Zang, R. Farnood, Effects of hydrogen peroxide concentration and ultraviolet light intensity on methyl *tert*-butyl ether degradation kinetics, Chem. Eng. Sci. 60 (2005) 1641–1648.

[22] S.K. Winnike-McMillan, Q. Zhang, L.C. Davis, L.E. Erickson, J.L. Schnoor, Phytoremediation of methyl *tertiary*-butyl ether, Phytoremediation (2003) 805–828.

[23] A. Burbano, D. Dionysiou, M. Suidan, T. Richardson, Chemical destruction of MTBE using Fenton's reagent: effect of ferrous iron/hydrogen peroxide ratio, Water Sci. Technol. 47 (2003) 165–171.

[24] A.A. Burbano, D.D. Dionysiou, M.T. Suidan, T.L. Richardson, Oxidation kinetics and effect of pH on the degradation of MTBE with Fenton reagent, Water Res. 39 (2005) 107–118.

[25] J.W. Kang, M.R. Hoffmann, Kinetics and mechanism of the sonolytic destruction of methyl *tert*-butyl ether by ultrasonic irradiation in the presence of ozone, Environ. Sci. Technol. 32 (1998) 3194.

[26] A.A Burbano, D.D. Dionysiou, T.L. Richardson, M.T. Suidan, Degradation of MTBE Intermediates using Fenton's reagent, J. Environ. Eng. 128 (2002) 799–805.

[27] X.-R. Xu, Z.-Y. Zhao, X.-Y. Li, J.-D. Gu, Chemical oxidative degradation of methyl *tert*-butyl ether in aqueous solution by Fenton's reagent, Chemosphere 55 (2004) 73–79.

[28] J.A. Bergendahl, T.P. Thies, Fenton's oxidation of MTBE with zero-valent iron, Water Res. 38 (2004) 327–334.

[29] G.V. Buxton, C.L. Greenstock, W.P. Helman, A.P. Ross, Critical review of rate constants for reactions of hydrated electrons, hydrogen atoms and hydroxyl radicals ($^{\bullet}OH/^{\bullet}O^-$) in aqueous solution, J. Phys. Chem. Data 17 (1988) 513.

[30] C. Walling, Fenton's reagent revisited, Accounts Chem. Res. 8 (1975) 125.

[31] B.A. Roe, A.T. Lemley, Treatment of two insecticides in an electrochemical Fenton system, J. Environ. Sci. Health B B32 (1997) 261.

[32] J. Pratap, A.T. Lemley, Electrochemical peroxide treatment of aqueous herbicide solutions, J. Agric. Food Chem. 42 (1994) 209.

[33] J. Pratap, A.T. Lemley, Fenton electrochemical treatment of aqueous atrazine and metolachlor, J. Agric. Food Chem. 46 (1998) 3285–3291.

[34] A.J. Bard, R.J. Parsons, J., Standard Potential in the Aqueous Solution, IUPAC, 1985.

[35] D. Pletcher, F.C. Walsh, Industrial Electrochemistry, Chapman and Hall, New York, 1989.

[36] D.A. Saltmiras, A.T. Lemley, Degradation of ethylene thiourea (ETU) with three Fenton treatment processes, J. Agric. Food Chem. 48 (2000) 6149–6157.

[37] F. Haber, J.J. Weiss, The catalytic decomposition of hydrogen peroxide by iron salts, Proc. R. Soc. Lond. Ser. A A147 (1934) 332.

[38] J.J. Pignatello, D. Liu, P. Huston, Evidence for an additional oxidant in the photoassisted Fenton reaction, Environ. Sci. Technol. 33 (1999) 1832.

[39] S.H. Bossmann, E. Oliveros, S. Goeb, S. Siegwart, E.P. Dahlen, L. Payawan Jr., M. Straub, M. Woerner, A.M. Braun, New evidence against hydroxyl radicals as reactive intermediates in the thermal and photochemically enhanced Fenton reactions, J. Phys. Chem. 102 (1998) 5542.

[40] M.L. Kremer, "Complex" versus "free radical" mechanism for the catalytic decomposition of hydrogen peroxide by ferric ions, Int. J. Chem. Kinet. 17 (1985) 1299.

[41] M.L. Kremer, G. Stein, Catalytic decomposition of hydrogen peroxide by ferric perchlorate, Trans. Faraday Soc. 55 (1959) 959.

[42] D.T. Sawyer, A. Sobkowiak, T. Matsushita, Metal [ML*x*; M = Fe, Cu, Co, Mn]/hydroperoxide-induced activation of dioxygen for the oxygenation of hydrocarbons: oxygenated Fenton chemistry, Acc. Chem. Res. 29 (1996) 409.

[43] C. Walling, Intermediates in the reactions of Fenton type reagents, Acc. Chem. Res. 31 (1998) 155.

[44] P.A. MacFaul, D.D.M. Wayner, K.U. Ingold, A radical account of "oxygenated Fenton chemistry", Acc. Chem. Res. 31 (1998) 159.

[45] B.V. Loffe, A.G. Vitenberg, Head-space Analysis and Related Method in Gas Chromatography, Wiley–Interscience, New York, 1983.

[46] S. Hong, C.M. Dutterweiler, A.T. Lemley, Analysis of methyl *tert*-butyl ether and its degradation products by direct aqueous injection onto gas chromatography with mass spectrometry or flame ionization detection systems, J. Chromatogr. A 857 (1999) 205.

[47] J. Grant, Sutton's Volumetric Analysis, 13th ed., Butterworths Scientific Publications, London, 1955.

[48] D.W. King, Role of carbonate speciation on the oxidation rate of Fe(II) in aquatic systems, Environ. Sci. Technol. 32 (1998) 2997.

[49] C. Walling, G.M. El-Taliawi, Fenton's reagent. II. Reactions of carbonyl compounds and α,β-unsaturated acids, J. Am. Chem. Soc. 95 (1973) 844.

[50] P. Neta, R.E. Huie, A.B. Ross, Rate constants for reactions of peroxyl radicals in fluid solutions, J. Phys. Chem. Ref. Data 19 (1990) 413.

[51] M.I. Stefan, J.R. Bolton, Reinvestigation of the acetone degradation mechanism in dilute aqueous solution by the UV/H_2O_2 process, Environ. Sci. Technol. 33 (1999) 870.

[52] M.I. Stefan, A.R. Hoy, J.R. Bolton, Kinetics and mechanism of the degradation and mineralization of acetone in dilute aqueous solution sensitized by the UV photolysis of hydrogen peroxide, Environ. Sci. Technol. 30 (1996) 2382.

[53] Q. Wang, A.T. Lemley, Kinetic model and optimization of 2,4-D degradation by anodic Fenton treatment, Environ. Sci. Technol. 35 (2001) 4509–4514.

[54] M. Lazar, J. Rychly, V. Klimo, P. Pelikan, L. Valko, Free Radical in Chemistry and Biology, CRC Press, Boca Raton, FL, 1989.

[55] K.D. Asmus, H. Möckel, A. Henglein, Pulse radiolytic study of the site of hydroxyl radical attack on aliphatic alcohols in aqueous solution, J. Phys. Chem. 77 (1973) 1218.

[56] R. Lesclaux, Combination of Peroxyl Radicals in the Gas Phase, John Wiley & Sons, Chichester, England, 1997.

[57] C. Von Sonntag, H.-P. Schuchmann, Peroxyl Radicals, John Wiley & Sons, Chichester, England, 1997.

[58] C. Von Sonntag, H.-P. Schuchmann, Elucidation of peroxyl radical reactions in aqueous solution with radiation chemistry technology, Angew Chem. Int. Ed. Engl. 30 (1991) 1229–1253.

[59] B.C. Gilbert, P.D.R. Marshall, R.O.C. Norman, N. Pineda, P.S. Williams, Electron spin resonance studies. Part 61. The generation and reactions of the *tert*-butoxyl radical in aqueous solution, J. Chem. Soc. Perkin Trans. 2 (10) (1981) 1392.

[60] J. March, Advance Organic Chemistry Reactions, Mechanisms and Structure, 4th ed., John Wiley & Sons, New York, 1992.

[61] P. Onstein, M.I. Stefan, J.R. Bolton, Competition kinetics method for the determination of rate constants for the reaction of hydroxyl radicals with organic pollutants using the UV/H$_2$O$_2$ advanced oxidation technology: the rate constants for the *tert*-butyl formate ester and 2,4-dinitrophenol, Adv. Oxid. Technol. 4 (1999) 231.